Activity Report of the LNF Detector Development Group - DDG

G. Bencivenni (Resp.), E. De Lucia, G. Felici, M. Giovannetti (Dott.), G. Morello, M. Poli Lener
in collaboration with
"LNF-SEA" D. Di Bari (Tecn.), M. Gatta (Tecn.), G. Papalino (Tecn.)
"LNF-Supporto agli Esperimenti" E. Paoletti (Tecn.), R. Tesauro(Tecn.)

1 Introduction

The Detector Development Group (DDG) has long been involved in the R&D, design and manufacture of classical gaseous detectors (Plastic Streamer Tube, Glass Spark Counters, Large Drift Chamber) and MPGDs for large high energy physics experiments. In particular the R&D activity on MPGDs (GEMs and innovative architectures) has been performed for the last twenty years in the framework of the LHCb experiment (CERN) with the development of the planar GEM detectors for the muon triggering and successively in the design and construction of the Cylindrical-GEM detectors for the Inner Tracker of the KLOE-2 experiment at DAFNE (LNF). At the moment the DDG is mainly involved in the R&D of the micro-Resistive WELL (μ-RWELL) detector for the phase-2 upgrade of the Muon system at LHCb. Exploiting the experience on the Diamond-Like-Carbon (DLC) deposition on Apical® foils, gained in the R&D on resistive MPGD, we recently promote the development of the surface RPC (sRPC), an innovative RPC concept based on surface resistive electrodes. Recently the group has been involved on thermal neutron detectors development, based on both μ-RWELL and sRPC technology. In this framework a DC Magnetron sputtering machine (co-funded with the CERN MPT workshop) for DLC and B4C deposition on Apical foils has been recently acquired. The group is also active on MPGDs and sRPCs technology transfer to industry. In the following the main achievements of the 2022 on the main research lines are reported:

- μ-RWELL for high rate environment (LHCb)
- μ-RWELL for tracking (RD-FCC)
- μ-RWELL for tracking (Low-mass Cylindrical-μ-RWELL for Inner Trackers at Super-Charm-Tau-Factories)
- development of thermal neutron detectors (URANIA-V)
- development of surface Resistive Plate Counters.

2 μ-RWELL for high rate environment - LHCb

The μ-RWELL technology [1)] is envisaged to realise the innermost regions of the muon detection system for the phase-II upgrade of the LHCb experiment at the High Luminosity LHC (HL-LHC). The detector will be installed during the Long Shutdown 4 of the LHC (LS4), and it will start data taking during Run 5, currently scheduled for 2032.
In the 2022, the R&D program was focused on the study of a new high-rate μ-RWELL layout,

called PEP (Patterning-Etching-Plating). This layout, recently introduced as a synthesis of the already tested high-rate layouts, (figure 1) is based on a single DLC layer high-rate scheme.
In this layout the grounding connection of the DLC is performed creating a conductive grooves by etching from the top Cu layer of the base material (where also the amplification stage is realised) through the Kapton® foil down to the DLC. The name PEP is the acronyms of the three main processes involved in the production of this layout:

- Patterning – the top copper is patterned to expose thin lines of Kapton®: these lines will become the ground connections (the central 50 µm wide zone in figure 1).
- Etching – the exposed Kapton® is etched, creating long grooves in the detector. The rest of the active area is protected thanks to the Copper (that in this phase acts like a protective mask).
- Plating – the groove is filled by screen-printing technique with silver glue, that sticks to the DLC. Then it is possible to create a plating between the two conductors: the top Cu and the silver glue.

After the creation of the groove connections, usually referred with a synecdoche as "PEP" or "PEP lines", it is possible to proceed with the usual step to create the amplification holes. A crucial aspect is to separate the top copper from the PEP line: usually the former is connected to HV while the latter to ground, in order to have the amplification field inside the blind holes.

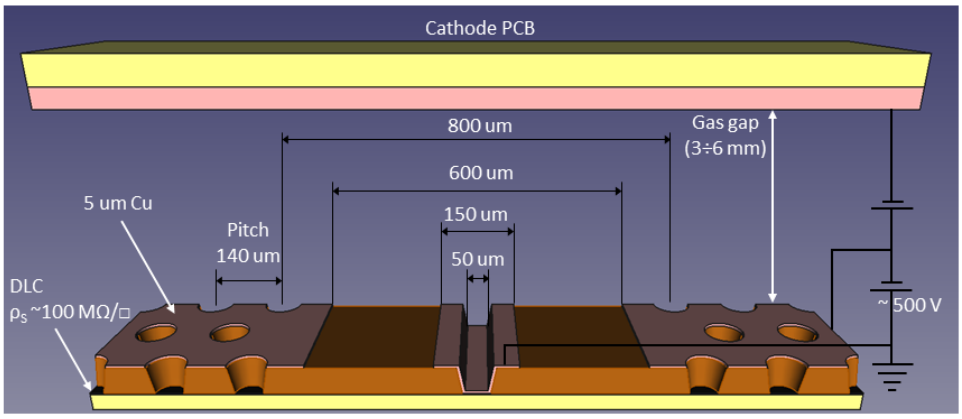

Figure 1: Sketch of the Patterning-Etching-Plating (PEP) layout.

Along the optimisation process of the layout the geometrical parameters of the PEP has been tuned. As reported in table 1 at least three major sub-versions have been realised. Here follows a brief description of the changes:

- in the PEP0 the grounding lines inside the active area started as a prong (or comb-like) structure. While the PEP1 inherit this design, the PEP2 has now only straight lines.
- In the PEP0 the distance between the top copper, connected to HV, and the PEP plated connection, at ground, could lead to instabilities similar to the ones observed in MSGC. Detectors from the PEP1 version, increasing the distance between these two parts, were able to achieve gain larger than 8000 without showing any instabilities.
- The DOCA and the ground pitch were changed in order to obtain a geometrical acceptance

of the detector larger than 90 %.

Table 1: Different PEP geometrical parameters.

Layout	Ground pitch [mm]	PEP-TOP separation [mm]	Dead zone [mm]	DOCA [mm]	Geometric Acceptance [%]
PEP0	6 // 8	0.115	1	0.475	66 %
PEP1	6 // 8	0.225	1	0.475	66 %
PEP2.1	8.9	0.255	0.8	0.375	91 %
PEP2.2	17.8	0.255	0.8	0.375	95.5 %

The gas gain and the rate-capability for PEP2 prototypes has been measured with an X-ray gun and are reported in figures 2 and 3.

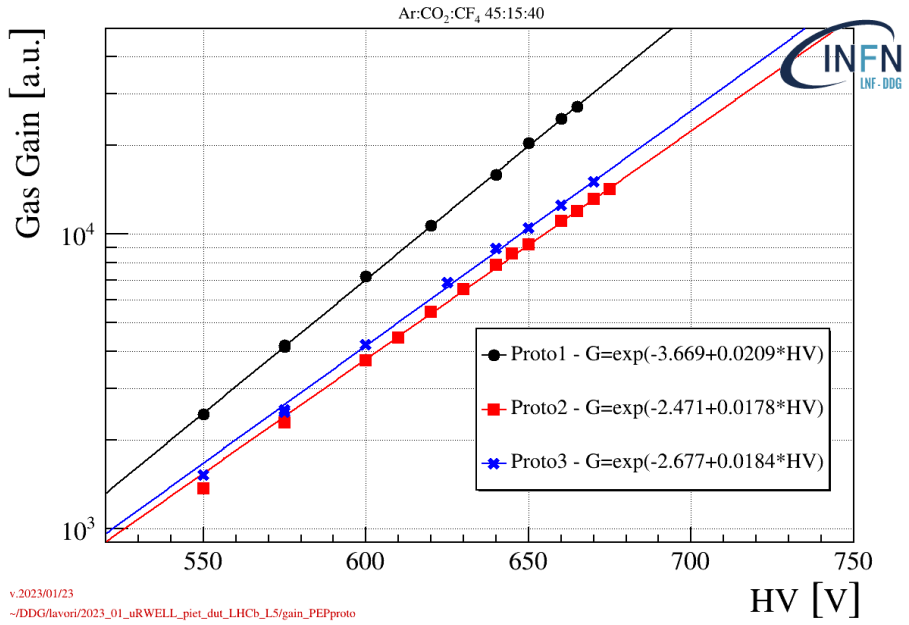

Figure 2: Gain calibration for three PEP2.1 prototypes in Ar:CO_2:CF_4 45:15:40.

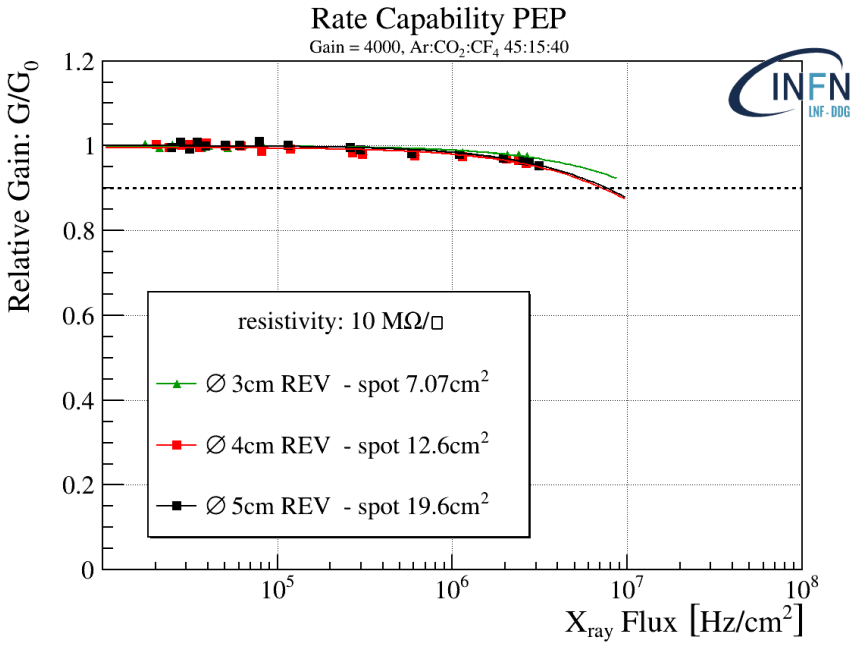

Figure 3: Normalised gain for the PEP as a function of the X-ray flux and different beam spot at a nominal gas gain of 4000.

3 μ-RWELL for tracking - FCC-ee

Due to its fine tracking capability the μ-RWELL is proposed as active sensor for the muon detection system and the pre-shower of the IDEA detector concept [2] designed for the FCC-ee [3] and CEPC [4] future large circular leptonic colliders.

The spatial performance of resistive MPGDs in general depends on the surface resistivity of their resistive stage as well as the strip pitch of the readout board. The results of a preliminary study of the cluster size and spatial resolution dependence on different DLC resistivity are reported in figure 4a and figure 4b respectively. In the 2022, the R&D program on the μ-RWELL detectors as tracking device has been focused to study the performance as a function of the strip pitch of the readout. A set of detectors with a strip pitch of $[0.4, 0.8, 1.2, 1.6]$ mm has been produced. The DLC surface resistivity of all detectors was around 40 MΩ/□, while the strip width was 150 μm. All these detectors have been exposed in October 2022 to a muon/pion beam at the CERN SPS. The setup has been composed of two trigger scintillators and two tracking stations each consisting of μ-RWELL with one-dimensional strip readout in X and Y coordinate. All gaseous detectors have been operated in Ar:CO_2:CF_4 45:15:40 at atmospheric pressure and were read-out with APV [5] front-end cards, interfaced by the Scalable Readout System. The APV chip, supplying analog output signals, allows the study of the detector tracking performance based on the charge centroid method.

As shown in figure 5a, the total charge collected on the readout strips decreases with the increase of the strip pitch. The hypothesis is that, since the strip width is the same for all detectors under test

(150 µm), when the strip pitch increases part of the signal that should be collected on the readout strips is "lost". Since the induction of the signal depends on the capacitive coupling between the DLC stage and the readout strip (for strip electrodes), and the capacitive coupling between the DLC and the top (for top electrode), it seems that when the strip pitch increases part of the signal that should be collected on the readout strips is induced on the top µ-RWELL electrode. The correct interpretation of this effect will require the development of a model of the coupling of the readout scheme with the amplification stage through the resistive layer, currently not available. The cluster size distribution, as expected, shows that increasing the strip pitch the number of fired strips sensibly decreases, tending to a cluster size very close to 1, figure 5b. In agreement with the decrease of the total collected charge, a strip pitch increase results in a shift at higher HV of the efficiency knee, figure 5c. The spatial resolution, figure 5d, is clearly affected by the strong dependence of the cluster size on the strip pitch. Indeed increasing the strip pitch the spatial resolution tends to the limit pitch/$\sqrt{12}$, and only with the high granularity readout (0.4 mm strip pitch) a spatial resolution better than 100 µm is achieved.

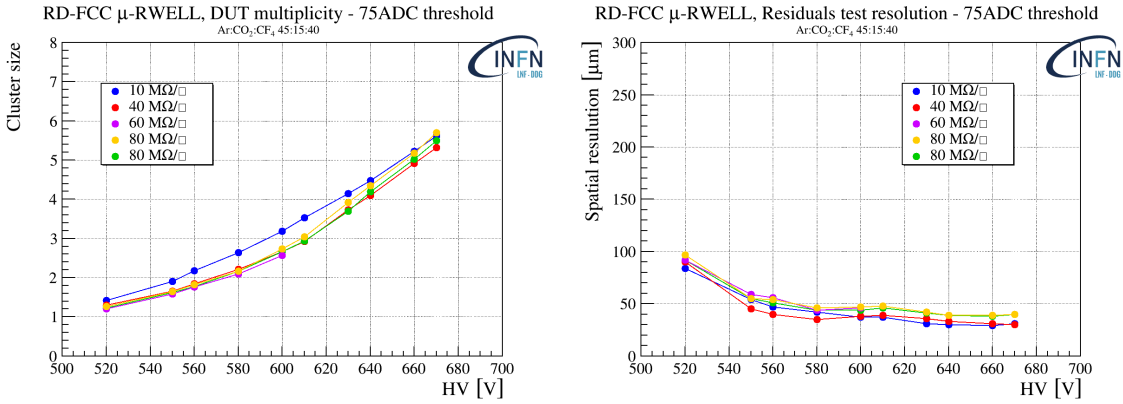

(a) Strip cluster size as a function of the HV.

(b) Residuals as a function of the HV.

Figure 4: Results of the DLC resistivity scan test campaign.

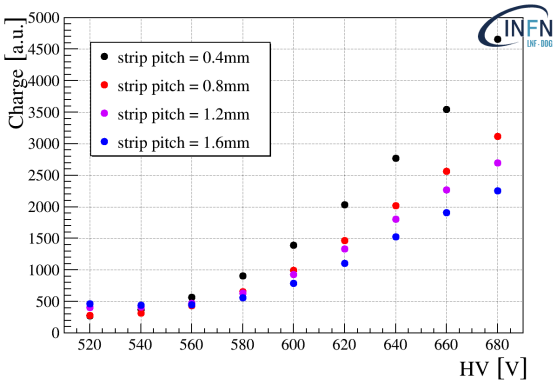

(a) Cluster charge for different HV.

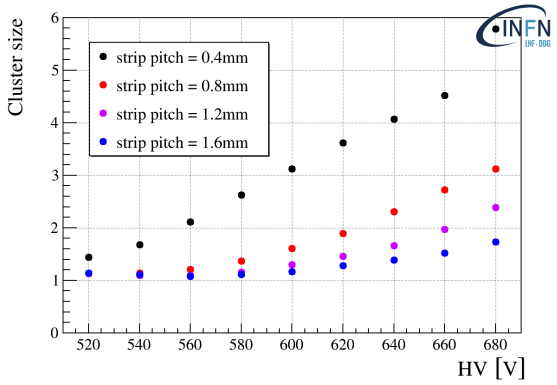

(b) Strip cluster size for different HV.

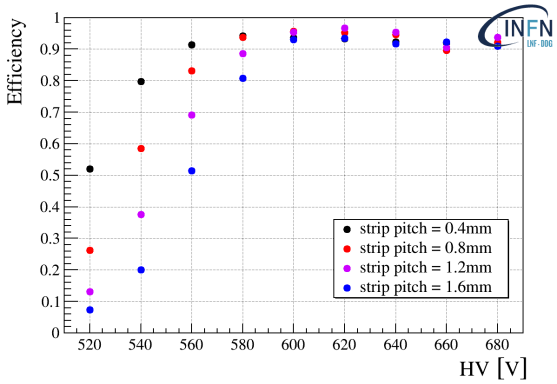

(c) Tracking efficiency for different HV.

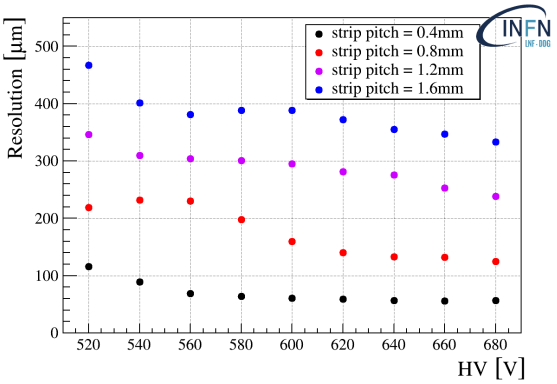

(d) Residuals width for different HV.

Figure 5: Results of the pitch scan test campaign.

4 Low-mass Cylindrical-μ-RWELL as Inner Trackers for Super-Charm-Tau-Factories

The idea of the cylindrical μ-RWELL (C-RWELL) as a low mass Inner Tracker (IT), has been developed in the framework of the R&D for future high luminosity $e^+ - e^-$ colliders with a centre of mass energy around 10 GeV (Super-Charm-Tau-Factories - SCTF). The main requirement for an IT at relatively low energy colliders is to reduce as much as possible the multiple scattering of the out-coming particles with the structures of the detectors, decreasing then systematic errors on reconstructed tracks, and consequently on the vertex reconstruction.

In the 2022 the activity has been focused on the design and construction of the main components of the C-RWELL prototype. The idea was to realise a modular detector which can be open in case of malfunctioning. The main feature of the μ-RWELL is to have the amplification stage, the resistive layer and the readout board embedded in one single element. The possibility to realise this element with flexible substrates makes the technology suitable for non-planar geometry. Two ideas of C-RWELL have been studied, both based on a common double-faced cathode layout. In

one case (figure 6) a two large radial gaps option for a 10 cm global sampling gas along the radial direction has been considered, while in the second case (figure 7) four thinner gaps for a 4 cm global sampling gas are foreseen.

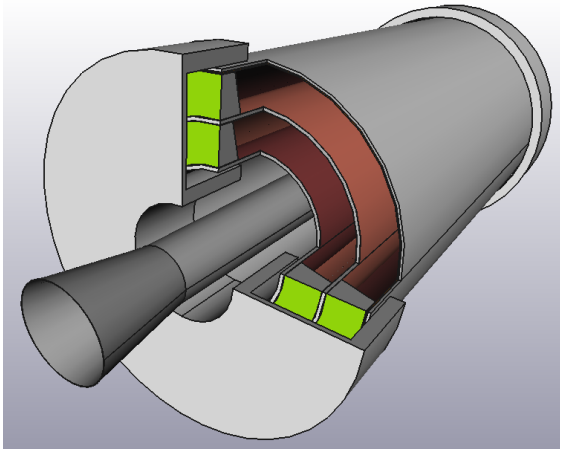

Figure 6: Double large gas gaps (10 cm global sampling gas) IT option.

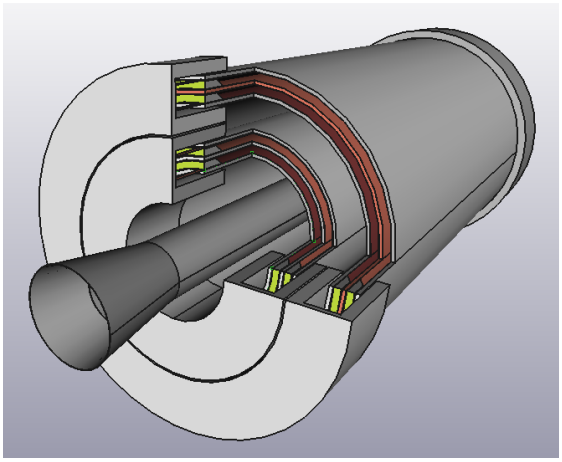

Figure 7: Pair of double thinner gas gaps (4 cm global sampling gas) IT option.

Depending on the materials choice the two layouts could be realised with a global material budget respectively in the range of $0.75 \div 0.86\,\%$ X0 and $1.46 \div 1.72\,\%$ X0. For both layouts, the cylindrical μ-RWELL_PCB is divided in three "roof tiles" detectors (figure 8) that, thanks to the possibility to open (and re-close) the cylindrical support, are removable in order to be replaced in case of malfunctioning.

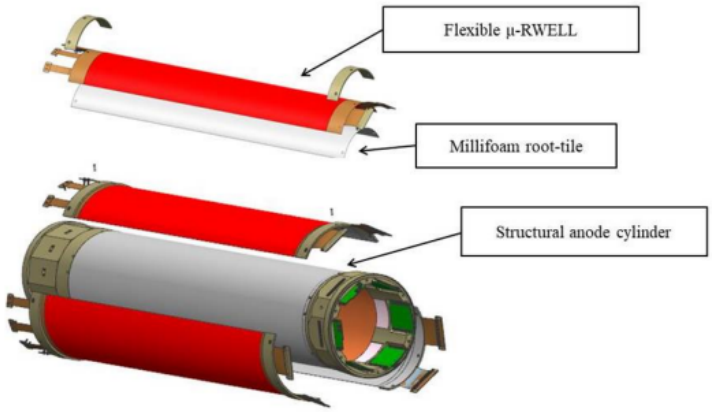

Figure 8: Sketch of the assembly of the three roof-tile detectors on the anode cylinder. The anode cylinder is made of composite material: an FR4–Millifoam®–FR4 sandwich plus an additional finely machined layer of Millifoam®.

A 1 cm large mono-gap prototype, composed of coaxial cylindrical anode and cathode structures, has been designed: the dimensions and all relevant numbers of the prototype are summarised in table 2.

Table 2: Dimensions and relevant numbers of the C-RWELL prototype.

Anode ⌀ [mm]	Cathode ⌀ [mm]	Drift gap [mm]	Active length [mm]	r/out chs	strip pitch [mm]
168.5	188.5	10	600	768	0.680

The mechanical components of the prototype have been realised by the LOSON S.r.l., a company with a remarkable expertise in composite materials. The cathode, 9, is the outermost electrode of the prototype, it has been laminated starting from a $50 + 5$ µm thick Kapton® +Cu foil glued on a 100 µm thick skin of fiber-glass, a layer of a 3 mm thick Millifoam®. A second fiber-glass skin and a copper layer, acting as Faraday cage, complete the cathode stack. The flanges at the two ends of the cathode are made of PEEK.

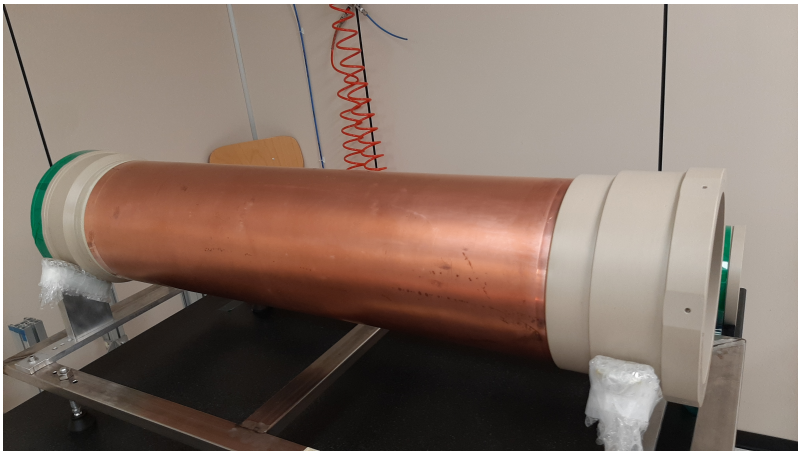

Figure 9: the cylindrical cathode of the C-RWELL

The cylindrical anode is composed of three roof-tiles, each covering 120°. Each flexible µ-RWELL_PCB, designed at LNF and built at the CERN-MPT-DT Workshop, is equipped with axial strips parallel to the axis of the cylinder, figure 10. The µ-RWELL_PCB is then glued on the roof-tile support, realised with a 3 mm (0.02 % X0) thick Millifoam®.

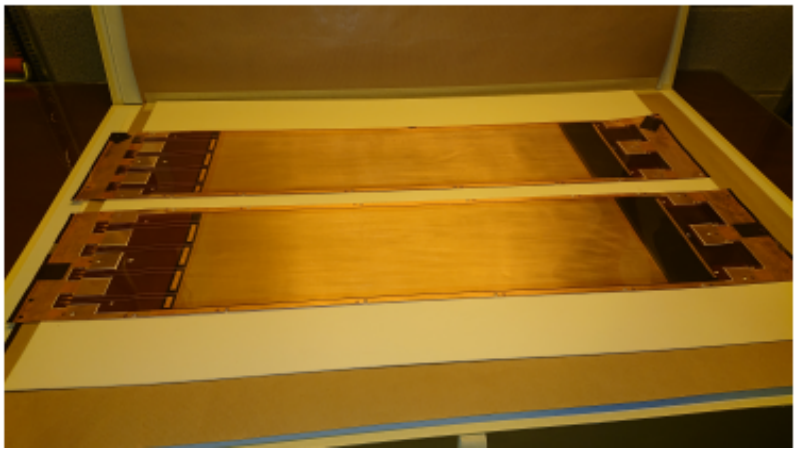

Figure 10: The μ-RWELL_PCB tiles of the C-RWELL

The production of flexible μ-RWELL tiles has been completed and the final assembly of the whole detector will be performed in the 2023. The first roof-tile has been assembled to the structure, as a first test for the final procedure, 11. Once the detector will be completed a cosmic ray test using APV25 FEE is foreseen.

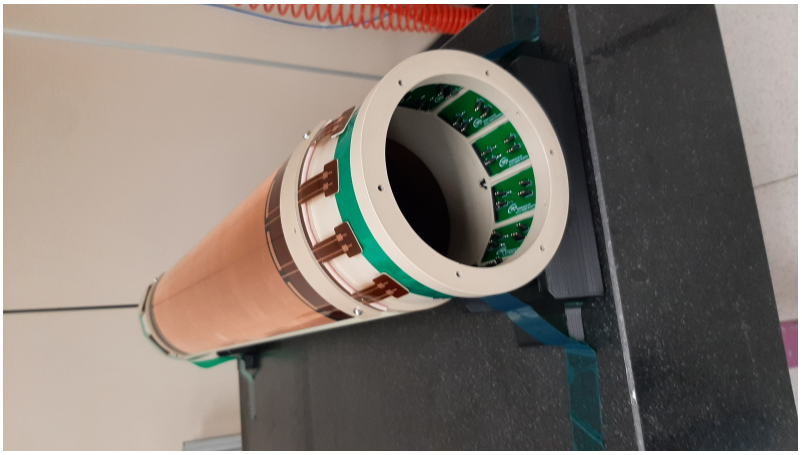

Figure 11: The C-RWELL anode with the first μ-RWELL tile assembled

5 Thermal neutron detectors - URANIA-V project

The μ-RWELL technology finds room for further applications, even aside HEP: for example in neutron conversion, possible if the detector is equipped with a proper converter. In fig. 12 the neutron absorption is reported for different materials as a function of their kinetic energy. For many years neutron detectors have exploited the high cross-section of neutrons with ^{3}He. Nevertheless in the latest years a shortage of this element increased its cost, involving as a consequence a large impact on the neutron detector production.This element is not extracted by natural resources but it is of industrial origin, precisely stemming from the decay of tritium, hugely accumulated

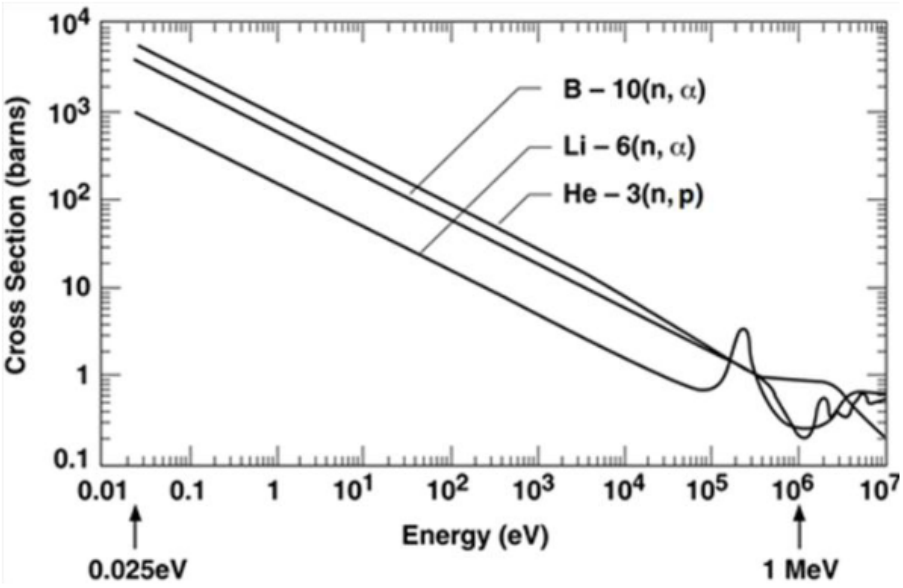

Figure 12: Neutron absorption cross sections for several isotopes as a function of incident neutron kinetic energy.

during the Cold War to boost the nuclear weapons. At present days the heavy production of neutron detection for homeland security and the reduced interest in collecting tritium, thanks to the nuclear warheads anti-proliferation treaties between Russia and USA after the official end of the Cold War[1], addressed the shortage[2] of the ^{3}He. Looking at fig. 12, boron is a suitable candidate as a converter for neutrons. For thermal neutrons the expected reactions are

$$\mathrm{n}+^{10}\mathrm{B}\rightarrow\begin{cases}\alpha\,(1.78\,\mathrm{MeV})+^{7}\mathrm{Li}\,(1.02\,\mathrm{MeV}) & 6\%\\ \alpha\,(1.47\,\mathrm{MeV})+^{7}\mathrm{Li}\,(0.84\,\mathrm{MeV})+\gamma\,(0.48\,\mathrm{MeV}). & 94\%\end{cases} \tag{1}$$

This element can be actually deposited by means of magnetron sputtering machines. In the case of the μ-RWELL technology the boron is sputtered on the surface of the cathode, thus obtaining a converter embedded in the active volume of the detector. At least one of the two charged particles is emitted towards the gas gap. An optimisation of the Boron thickness is necessary to achieve a good compromise between the conversion efficiency and the transparency for the charged particles since these latter could be indeed re-absorbed in the boron itself. GEANT4 simulations played a remarkable role in this task (fig. 13). To increase the amount of converter different solutions have been adopted: cathodes with non-planar profiles and coated meshes inserted between the cathode and the amplification stage of the detector. Also in this case we benefit from the simulations, using the outcome of GEANT4 as input to GARFIELD++, since with the new elements there could be inefficiency related to fractions of active volume with low drift field and/or obstacles for the electrons produced by the ionisation. Anyway, due to the limited kinetic energy of the particles, the

[1]In particular the new START (STrategic Arms Reduction Treaty) ratified in 2011 and expected to last until 2026

[2]https://sgp.fas.org/crs/misc/R41419.pdf

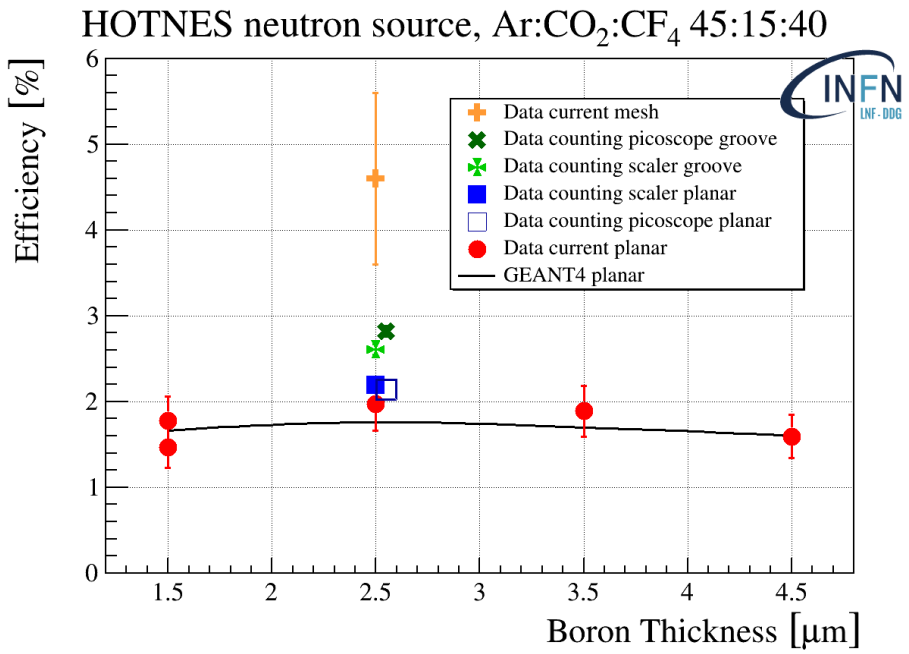

Figure 13: Summary results of the HOTNES data campaign. As a reminder, the efficiency for 25 meV is twice the one showed in figure, due to the higher neutron cross section for that energy.

average ionisation[3] is about four orders of magnitude larger than what expected for a m.i.p.. For this reason the detector is operated at a gain below 1000, then intrinsically excluding the photon detection (background). The simulations have been validated with two data taking campaigns carried out at the ENEA-Frascati HOTNES facility, where a ^{241}Am-B source is placed at the bottom of a polyurethane pit draw to ensure an almost uniform particle fluence (750 Hz/cm^2) at a distance of 20 cm. The data reported in fig. 13 have been recorder with two methods: counting mode (using a picoscope amplifier) and in current mode. It is quite clear how the new geometry of the cathode and the insertion of the coated mesh increase the detection efficiency.

Due to the compactness of the device, a final station can be realised as a stack of μ-RWELL, that, once OR-ed the signals, sums up the single detector efficiency. It seems then reliable to achieve an efficiency up to 20 %.

6 The surface Resistive Plate Counters

Standard Resistive Plate Counters (RPCs) are based on the use of at least one bulk resistivity electrode, typically made of bakelite [6], semiconductive [7] or float [8] glass, with a volume resistivity in the order of $\rho \sim 10^{10\div12}\,\Omega\cdot$cm. The avalanches produced by the passage of a particle, discharging a limited area around its location, are automatically quenched by the voltage drop on the resistive electrode. Such devices with 2 mm thick electrodes and $1 \div 2$ mm gas gap, when

[3]The energy distribution of the emitted particles is nearly flat from few keV to the maximum energy reported in eq. 1.

operated with dense gas mixtures at atmospheric pressure, exhibits a time resolution of about 1 ns. The presence of resistive electrodes affects the rate capability of the detector due to the fact that the voltage recovery time around the dead zone is proportional to the volume resistivity and the electrodes thickness. Lowering the resistivity ρ and the thickness d of the electrodes is the standard recipe to achieve a sizeable increase of the detector rate capability. In the last decades several low volume resistivity materials have been tested allowing the construction of RPC standing radiation fluxes up to $7\,\mathrm{kHz/cm^2}$ [9].
The revolutionary approach[4] proposed by our group is to realise an RPC based on easily modulated surface resistivity electrodes manufactured with industrial DLC sputtering techniques on flexible or semi-rigid supports.

6.1 The sRPC layout

The electrodes of the sRPC prototype are shown in fig. 14. They consist of a 2 mm thick standard float glass sheet on which a suitably patterned Apical® foil sputtered with DLC has been glued. The range of DLC surface resistivity explored in the first phase of the R&D was $1 \div 20\,\mathrm{G\Omega/\square}$. The 2 mm gas gap between the electrodes is ensured by E-shaped spacers made of Delrin®, inserted without gluing at the edges of the glass supports fig. 15. The electrodes sandwich is then inserted in a fiber-glass box that acts as gas volume container. The gas flows along the module through inlet/outlet pipes located on lateral opposite sides of the box. The HV is applied to the DLC electrodes through DLC coated Kapton® tails reported on the external side of the glass sheets. On one of the two end-caps of the fiber-glass box two HV connectors are inserted in order to supply the voltage to the DLC electrodes. External strip-patterned boards are used to pick-up the induced signals, transmitted through the resistive electrodes. In all these layouts the DLC electrode can be realised with a simple conductive dot-like or a dense grid-like current evacuation scheme.

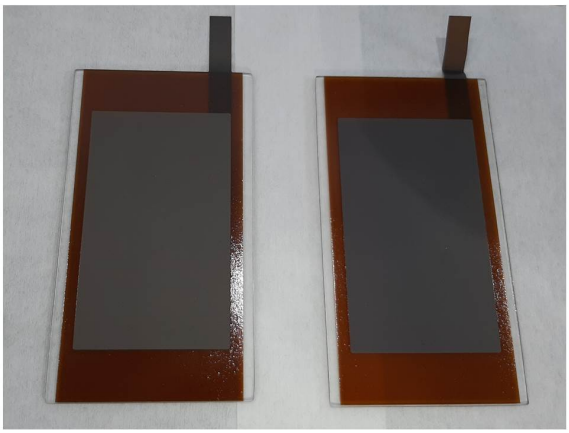

Figure 14: Glass sheets ($78\times140\,\mathrm{mm^2}$) with the DLC coated ($64\times120\,\mathrm{mm^2}$) Apical® foil electrodes.

[4]The idea of "*Timing detectors based on surface resistivity electrodes*" was patented in 2019 [10].

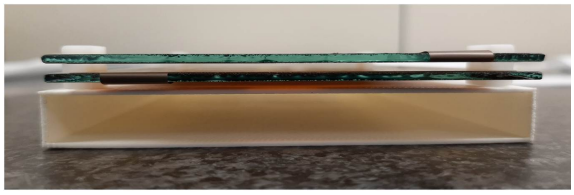

Figure 15: X-section of the sRPC electrodes coupled by E-spacers made of Delrin® (the internal tooth of the spacer is 2 mm thick).

All prototypes have been operated with the $C_2H_2F_4$:iC_4H_{10}:SF_6 93.5:5:1.5 gas mixture, while the FEE was based on the six-channels VTX pre-amplifier (with analog output and 10 mV/fC sensitivity).

6.2 The sRPC performance

As shown in fig. 16 the efficiency plateau curves of the first sRPC prototypes were not as large ($200 \div 300$ V) as the ones obtained with standard RPC with bulk resistivity electrodes (typically 1 kV). Instability effects correlated with a constant current drawn have been observed above a certain HV threshold, with consequent detector breakdown.

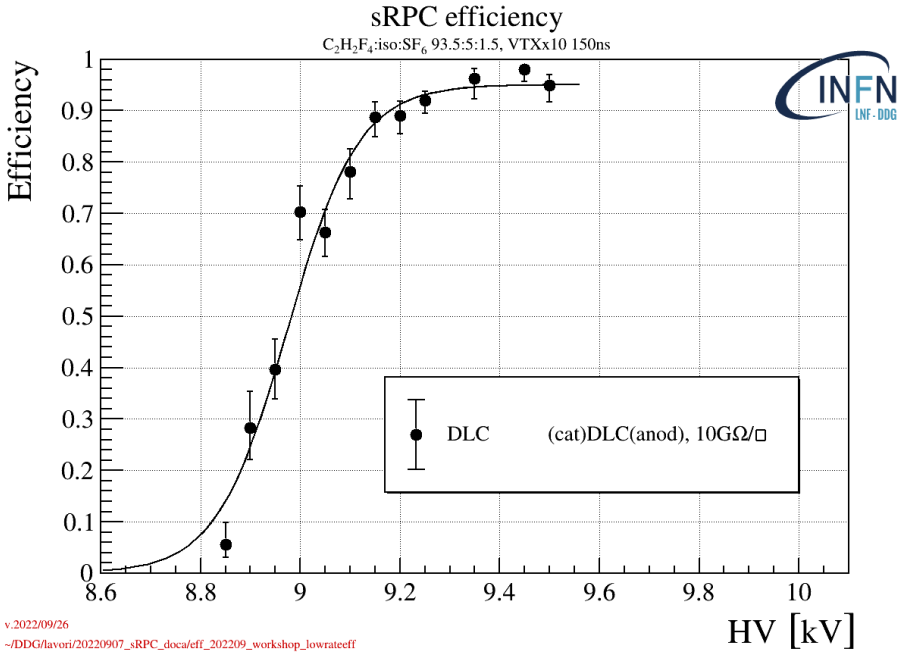

Figure 16: Efficiency curve for DLC(anode)-DLC(cathode) sRPC layout. Due to instability effects occurred around 9.5 kV a reduced plateau width of 250 V has been obtained.

The breakdown threshold is around 9.5 kV, corresponding to an electric field of ~ 45 kV/cm for a 2 mm gap. Considering that the DLC has a working function of few eV [11] and exhibits a non-negligible sensitivity to UV-photons [12], secondary electron emission due to photon-feedback

and/or field emission [13] may occur at the cathode surface. The electrons multiplied by the intense electric field within the gas gap can trigger a continuous current mode inducing a constant voltage drop through the electrodes, with a corresponding strong decrease of the electric field inside the gas gap such that no detectable signals are produced. In order to suppress secondary electrons extraction at the cathode surface a thin barrier on the cathode electrode could be an effective solution. Several coatings of the DLC cathode surface have been tested, among these the Licron® Crystal spray, a static dissipative coating with a $\rho \sim 10^{6 \div 9}\,\Omega \cdot \mathrm{cm}$ surface resistivity produced by the Techspray, led to positive results by significantly improving the stability of the detector. As shown in fig. 17 detectors with Licron® cathode passivation show an efficiency plateau of the order (or larger than) of 1 kV, while a long-term test to verify the detector stability is in progress.

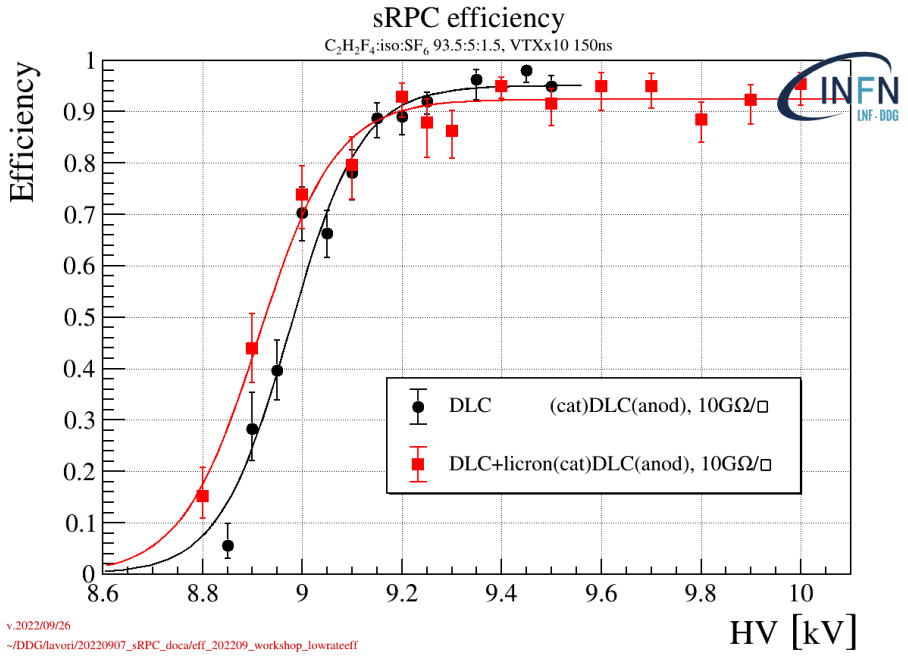

Figure 17: Comparison between DLC(anode)-DLC(cathode) and DLC(anode)-DLC(cathode-Licron®) efficiency curves.

Exploiting the experience gain on the R&D on μ-RWELL [14] we developed a first version of a HR electrode layout. As shown in fig. 18, a conductive grid with a pitch of $\sim 1\,\mathrm{cm}$ has been screen printed onto the DLC film. The DLC resistivity was $\sim 7\,\mathrm{G\Omega/\square}$. The rate capability of this layout has been measured with a 5.9 keV X-ray gun irradiating the prototype with spots with different size ($1 \div 5\,\mathrm{cm}$ spot diameter), larger than the pitch of the current evacuation grid of the electrodes (1 cm). As shown in fig. 19, a rate capability of $\sim 1\,\mathrm{kHz/cm^2}$ with X-ray has been measured.

Figure 18: DLC-HR electrodes. DLC resistivity is 7 GΩ/□, grid pitch 1 cm.

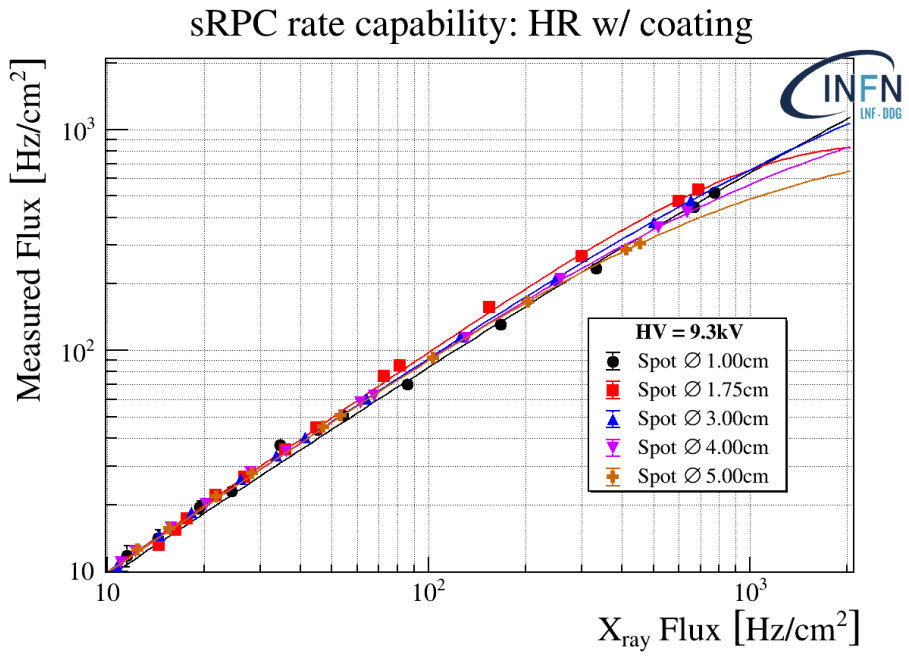

Figure 19: sRPC counts vs X-ray flux for different irradiation spot size.

7 List of Conference Talks by DDG - LNF Authors in Year 2022

1. G. Bencivenni et al., The surface Resistive Plate Counter: A new RPC based on resistive MPGD technology, presented at the Vienna Conference on Instrumentation, Feb 21 – 25, 2022, Vienna University of Technology, proceeding published on Nuclear Inst. and Methods in Physics Research, A 1038 (2022) 166948.
2. G. Morello et al., The micro-RWELL detector for the phase-2 upgrade of the LHCb muon system, presented at the 15^th Pisa Meeting on Advanced Detectors, La Biodola, Isola d'Elba,

May 22-28, 2022, proceeding published on Nuclear Inst. and Methods in Physics Research, A 1049 (2023) 168075.
3. G. Bencivenni et al., The surface Resistive Plate Counter: an RPC based on resistive MPGD technology, presented at the 15^th Pisa Meeting on Advanced Detectors, La Biodola, Isola d'Elba, May 22-28, 2022, proceeding published on Nuclear Inst. and Methods in Physics Research, A 1046 (2023) 167728.
4. M. Giovannetti, The surface Resistive Plate Counter (sRPC): an MPGD technology based RPC, NIM 2023, 7^th International Conference on Micro Pattern Gaseous Detectors 2022, Rehovot, Israel.
5. M. Giovannetti, uRANIA: a micro-Resistive WELL for neutron detection, NIM(2022) 15^th Pisa Meeting on Advanced Detectors, La Biodola, Italy,
6. G. Morello et al., The micro-RWELL detector for the phase-2 upgrade of the LHCb muon system, presented at the 15^th Pisa Meeting on Advanced Detectors, ICHEP22, Bologna, July 6th-13th, to be published on PoS(ICHEP2022)339.
7. M. Poli Lener, The pre-shower and the muon detection system of the IDEA detector for CepC, Beijing, China.
8. M. Poli Lener, sRPC: an RPC based on resistive MPGD technology, 2022 IEEE NSS-MIC-RTSD, Milan, Italy.
9. G. Morello et al., The micro-RWELL detector for high rates applications, 2022 IEEE NSS-MIC-RTSD, Milan, Italy.
10. M. Poli Lener, The state of art of μRWELL technology, NIM 2023, 7^th International Conference on Micro Pattern Gaseous Detectors 2022, Rehovot, Israel.

8 Publications

1. R. Farinelli et al., The μ-RWELL technology at the IDEA detector, , 41^{st} International Conference on High Energy Physics (ICHEP2022), Bologna, Italy,
https://doi.org/10.22323/1.414.0333
2. G. Bencivenni et al., The surface Resistive Plate Counter: a novel RPC based on MPGD technologies, NIM (2022), 15^th Pisa Meeting on Advanced Detectors, La Biodola, Italy,
https://doi.org/10.1016/j.nima.2022.167728
3. R. Farinelli et al., The μ-RWELL technology for the preshower and muon detectors of the IDEA detector, NIM (2022), 15^th Pisa Meeting on Advanced Detectors, La Biodola, Italy,
https://doi.org/10.1016/j.nima.2022.167993
4. G. Morello et al., The micro-RWELL detector for the phase-2 upgrade of the LHCb Muon system, NIM (2022), 15^th Pisa Meeting on Advanced Detectors, La Biodola, Italy,
https://doi.org/10.1016/j.nima.2023.168075
5. G. Bencivenni et al., The Surface Resistive Plate Counter: A new RPC based on resistive MPGD technology, NIM A 1038 (2022), 16^th Vienna Conference on Instrumentation, Vienna, Austria,
https://doi.org/10.1016/j.nima.2022.166948

References

1. G. Bencivenni at al., *The micro-Resistive WELL detector: a compact spark-protected single amplification-stage MPGD*, JINST 10 (2015) P02008.

2. R. Aly et al., *First test-beam results obtained with IDEA, a detector concept designed for future lepton colliders*", Nucl. Instrum. Meth. A958 (2020) 162088.

3. Abada, A. et al., *FCC Physics Opportunities: Future Circular Collider Conceptual Design Report Volume 1*, Eur. Phys. J. C79 (2019) 474.

4. The CEPC Study Group, *CEPC Conceptual Design Report: Volume 2 - Physics & Detector*, arXiv:1811.10545 (2018).

5. M. Raymond et al., *The APV25 0.25 m CMOS readout chip for the CMS tracker*, IEEE Nucl. Sci. Symp. Conf. Rec. **2** (2000) 9/113.

6. R. Santonico, R. Cardarelli, *Development of Resistive Plate Counters*, Nucl. Instr. & Meth. **A 377** (1981) 187.

7. Yu. Pestov et al., *A spark counter with large area*, Nucl. Instr. & Meth. **93** (1971) 269.

8. M. Anelli et al., *Glass electrode spark counters*, Nucl. Instr. & Meth. **A 300** (1991) 572.

9. R. Cardarelli et al., *Performance of RPCs and diamond detectors using a new very fast low noise preamplifier*, 2013 JINST P01003.

10. G. Bencivenni, G. Morello, M. Poli Lener, *Brevetto Italia n.102020000002359, INFN (submitted the 10th Sept. 2019 - registered the 6th Feb. 2020) "Elettrodo piano a resistività superficiale modulabile e rivelatori basati su di esso.*

11. A. Valentini, RD51-NOTE-2020-006.

12. Kordas, et al., 15^th Vienna Conference on Instrumentation, Feb. 18-22, 2019.

13. S.A. Korff, Electron and Nuclear Counters, D. Van Nostrand Company -Inc, Fourth Avenue, New York, USA, 1955.

14. G. Bencivenni et al., *The micro-RWELL layouts for high particle rate*, 2019 JINST 14 P05014.